

Epitaxial Nd-doped α - $(\text{Al}_{1-x}\text{Ga}_x)_2\text{O}_3$ films on sapphire for solid-state waveguide lasers

Raveen Kumaran,^{1,*} Thomas Tiedje,² Scott E. Webster,¹ Shawn Penson,¹ and Wei Li¹

¹Advanced Materials and Process Engineering Laboratory, University of British Columbia, Vancouver, British Columbia V6T 1Z4, Canada

²Department of Electrical and Computer Engineering, University of Victoria, Victoria, British Columbia V8W 2Y2, Canada

*Corresponding author: raveen@phas.ubc.ca

Received September 14, 2010; accepted October 5, 2010;
posted October 13, 2010 (Doc. ID 135043); published November 9, 2010

Single-crystal aluminum–gallium oxide films have been grown by molecular beam epitaxy in the corundum phase. Films of the $(\text{Al}_{1-x}\text{Ga}_x)_2\text{O}_3$ alloys doped with neodymium have favorable properties for solid-state waveguide lasers, including a high-thermal-conductivity sapphire substrate and a dominant emission peak in the 1090–1096 nm wavelength range. The peak position is linearly correlated to the unit cell volume, which is dependent on film composition and stress. Varying the Ga–Al alloy composition during growth will enable the fabrication of graded-index layers for tunable lasing wavelengths and low scattering losses at the interfaces. © 2010 Optical Society of America

OCIS codes: 160.5690, 160.3380, 310.0310.

Solid-state lasers (e.g., Nd:YAG, Ti:sapphire) in the form of planar waveguides have the virtue of being more compact and more efficient than their bulk counterparts. The strong optical confinement possible in waveguides leads to lower threshold powers, whereas the planar geometry offers better heat extraction and integration with semiconductor devices [1]. Planar waveguides of popular bulk laser materials have been grown by several methods, including liquid phase epitaxy and pulsed laser deposition [2].

Molecular beam epitaxy (MBE) is a promising alternative deposition method capable of producing epitaxial films with precise composition and structure. It features nonequilibrium growth conditions involving the simultaneous deposition of elemental sources, which allows for new laser materials with single-site doping of Nd inaccessible by bulk crystal growth methods. We showed such an example with the growth of single-crystal Nd-doped sapphire films [3] ($\text{Nd}:\alpha\text{-Al}_2\text{O}_3$), a new material with optical gain comparable to Nd:YVO₄, which is one of the highest-gain solid-state lasers available. Here we present Nd: $\alpha\text{-Ga}_2\text{O}_3$ on sapphire, another new corundum-structure laser material with a higher refractive index than sapphire suitable for waveguiding. We also report single-crystal alloys of Nd-doped α - $(\text{Al}_{1-x}\text{Ga}_x)_2\text{O}_3$ suitable for making graded-index layers.

The films were grown on sapphire substrates in a VG-V80H MBE system modified by the addition of a high-throughput turbomolecular pump and a silicon carbide substrate heater [4]. Substrate preparation included furnace annealing at 1150 °C for 8 h to generate atomically flat terraces [4] and back-surface metallization to improve radiative coupling to the heater. Effusion cells loaded with elemental Ga, Al, and Nd sources were heated independently to generate the desired flux ratio. Nd₂O₃ powder was also tested successfully as a source material. During the growth campaign we used two different oxygen plasma sources: an in-house designed 200 W VHF helical resonator source and a customized 600 W commercial source from SVT Associates. The background oxygen pressure was typically 2×10^{-5} torr during growth.

$\alpha\text{-Ga}_2\text{O}_3$ was considerably more difficult to grow than sapphire because of desorption of the volatile suboxide

Ga₂O. Using the in-house plasma source, low substrate growth temperatures (500 °C) and low growth rates (0.5 nm/min) were necessary to minimize desorption while maintaining crystallinity. Switching to the SVT source running at 200 W produced high levels of atomic oxygen such that the group III metal flux became rate limiting. Higher growth rates up to 2 nm/min were then possible at temperatures up to 800 °C when the thermally stable $\beta\text{-Ga}_2\text{O}_3$ phase started to appear in addition to the α phase. The Nd-doping level was less than 1 at. % relative to the metal concentration.

We grew Nd-doped $\alpha\text{-Ga}_2\text{O}_3$ on R-, A-, and M-plane sapphire substrates. Films grown on the C-plane under similar conditions were entirely $\beta\text{-Ga}_2\text{O}_3$. In Fig. 1, we show three different types of x-ray diffraction (XRD) data for an Nd: $\alpha\text{-Ga}_2\text{O}_3$ film on A-plane sapphire. The x-ray data show that the film is single phase (no $\beta\text{-Ga}_2\text{O}_3$) and has the same crystal orientation as the substrate. From the film peaks in the $\theta/2\theta$ scan in Fig. 1(a), we find that the interplanar spacing normal to the substrate is 0.1% larger than that of bulk $\alpha\text{-Ga}_2\text{O}_3$ [5]. This lattice expansion may be due to compressive strain associated with the substrate lattice mismatch or structural defects in the film. The small broadening of the film peak in the reciprocal space map in Fig. 1(c) shows that the film has a slight mosaicity centered about the substrate orientation that is possibly an indication of columnar growth.

Since the films are single phase, the optical properties that we measured are unique to α -phase Nd:Ga₂O₃. The refractive index at a wavelength of 1 μm is 1.91 (compared with 1.75 for sapphire) as measured by broadband reflectance spectroscopy. With that index contrast, a 1-μm-thick core with sapphire cladding would be sufficient to confine 92% of the fundamental TE mode. Nd: $\alpha\text{-Ga}_2\text{O}_3$ is uniaxial like sapphire, with polarization-dependent emission either parallel or perpendicular to the hexagonal *c* axis (optic axis). We collected the emission while optically pumping the 823 nm absorption peak; the equivalent Nd: $\alpha\text{-Al}_2\text{O}_3$ peak is at 825 nm. The product of emission cross section σ and lifetime τ is a useful figure of merit for optical gain in a lasing material. We calculated $\sigma \cdot \tau$ from the emission spectra using the equation [6]

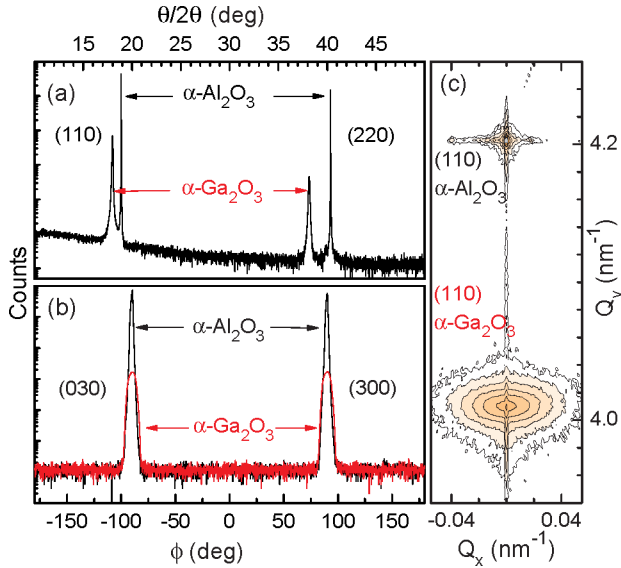


Fig. 1. (Color online) High-resolution x-ray diffraction from a 120-nm-thick Nd:α-Ga₂O₃ film grown on A-plane sapphire: (a) $\theta - 2\theta$ scan showing that the film is single phase. (b) ϕ rotation scans showing that the in-plane orientation of the film matches the substrate. ϕ scans involve detecting off-axis peaks while the sample is rotated about its normal. (c) Reciprocal space map indicating slight mosaicity as shown by the broad film peak. Q_x and Q_y refer to the in-plane and out-of-plane directions, respectively, and have units of inverse interplanar spacings.

$$\sigma_{\text{pol}}(\lambda) \cdot \tau = \frac{3\lambda^5 I_{\text{pol}}(\lambda)}{8\pi c n^2} \left[\int \{I_{\parallel}(\lambda) + 2I_{\perp}(\lambda)\} \lambda d\lambda \right]^{-1}, \quad (1)$$

where pol is the polarization, either \perp or \parallel to the optic axis, λ is the wavelength, n is the refractive index, and I is the emission intensity.

Figure 2 compares the $\sigma \cdot \tau$ of Nd:α-Ga₂O₃ to Nd:α-Al₂O₃. The narrow emission peaks are consistent with the high degree of structural order observed in the x-ray measurements. The emission from Nd:α-Ga₂O₃ is an almost identical yet blueshifted version of that from Nd:α-Al₂O₃, suggesting that the Nd³⁺ ion has the same local atomic structure in both materials except for the

larger Nd—O bond length in Nd:α-Ga₂O₃. The spectrum \parallel to the optic axis is dominant and has a strong emission peak at 1090 nm with a $\sigma \cdot \tau$ of 70×10^{-24} cm² s. For comparison, the 1064 nm peak of Nd:YAG has a $\sigma \cdot \tau$ of 60×10^{-24} cm² s [6]. The 1090 nm peak would likely be stronger if not for the higher degree of structural disorder relative to Nd:α-Al₂O₃, as shown by the wider FWHM and stronger background (see Fig. 2 inset).

The structural and optical similarity between the two isomorphs provided a compelling case to make oxide alloys. We grew a set of Nd-doped α -(Al_{1-x}Ga_x)₂O₃ films at 800 °C with the composition controlled by fixing the Ga flux and varying the Al fluxes. The Ga/Al ratio was measured postgrowth by x-ray photoelectron spectroscopy. Both XRD and photoluminescence measurements showed that the films were single crystal in the corundum structure. Figure 3 shows XRD data and photoluminescence (inset) as a function of the composition of the alloy films. Reciprocal space maps of the (300) off-axis peak indicate that both the in-plane and out-of-plane lattice constants approach Nd:α-Al₂O₃ with increasing Al content. As the unit cell shrinks, the dominant emission peak shifts continuously from 1090 to 1096 nm, as shown in the inset in Fig. 3.

When an epitaxial film is grown on a lattice mismatched substrate, the film is typically strained. The reciprocal space maps in Fig. 3 show that the Al-rich films are compressively strained in-plane to match the lattice constant of the sapphire substrate with a critical Ga content of $x = 0.4$. For higher Ga contents, the lattice constant of the film expands both in and perpendicular to the plane of the film. The in-plane expansion is presumably associated with the formation of bulk or interfacial structural defects in the film. The effect of the strain and the composition change on the emission wavelength is shown in Fig. 4 as a function of the Ga content.

To better understand the effect of the lattice strain on the emission wavelength, we calculated the volume of the hexagonal unit cell (Fig. 4 inset) using the lattice constants from Fig. 3 as well as from reciprocal space maps of the (226) off-axis peak. In Fig. 4, we show that the wavelength of the emission peaks is linearly correlated

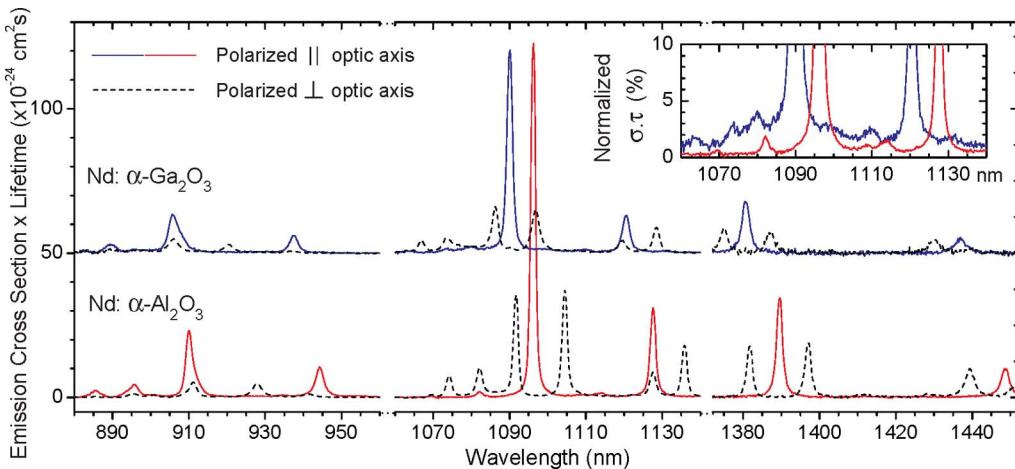


Fig. 2. (Color online) Product of emission cross section σ and lifetime τ for Nd-doped α -Ga₂O₃ and α -Al₂O₃ films grown on A-plane sapphire. $\sigma \cdot \tau$, which is proportional to optical gain, is calculated from the emission spectra using Eq. (1). The spectra are due to Nd³⁺ transitions from the $^4F_{3/2}$ manifold to the $^4I_{9/2}$, $^4I_{11/2}$, and $^4I_{13/2}$ manifolds, respectively. Inset, a magnified plot of normalized $\sigma \cdot \tau$ for emission-polarized \parallel optic axis.

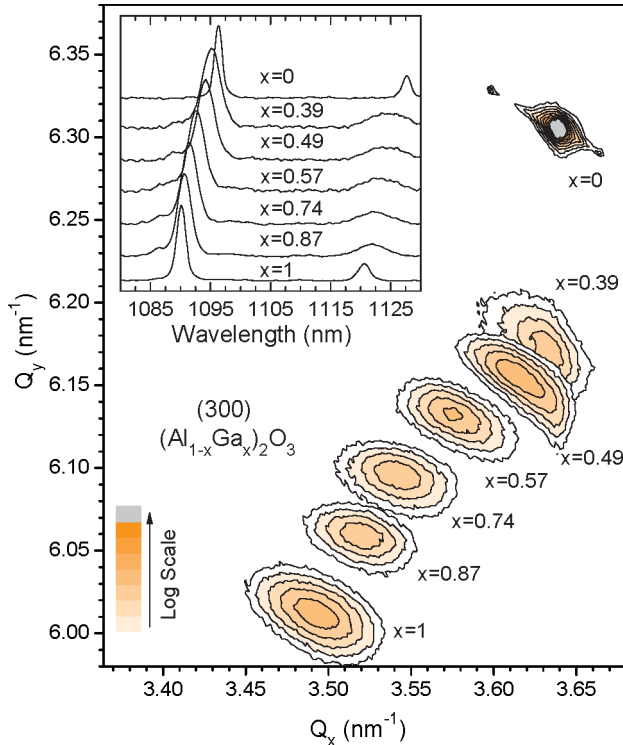


Fig. 3. (Color online) Reciprocal space map showing the off-axis (300) peaks for Nd-doped α -(Al_{1-x}Ga_x)₂O₃ films grown on A-plane sapphire. Film thicknesses range from 85 to 165 nm. Varying the composition results in the transition of film peaks from α -Ga₂O₃ to α -Al₂O₃ in Q_x and Q_y , which are the inverse interplanar spacings along the [110] (in-plane) and [110] (out-of-plane) directions, respectively. Al-rich films deviate from the expected linear trend, indicating that the films are compressively strained in-plane to match the substrate instead of being fully relaxed. Inset, the composition dependence of the strong emission peak (normalized).

to the unit cell volume. A strain dependence of the emission wavelength of almost a factor of 2 larger has been reported in bulk Nd:YVO₄ under hydrostatic pressure [7]. Physically this finding suggests that the change in pressure of the oxygen cage coordinating the rare-earth ion is the reason for the composition dependence of the emission wavelength.

Nd-doped α -(Al_{1-x}Ga_x)₂O₃ is a rare-earth doped binary oxide alloy useful for making compositionally tuned lasers. A wavelength range of 1090–1096 nm is accessible by compositional control of the unit cell volume. Single-phase laser alloys typically involve ternary oxides such as the Y₃(Ga_xAl_{1-x})₅O₁₂ garnets [8] and the (Y_xGd_{1-x})VO₄ vanadates [9]. The strong 1064 nm peak of the former does not shift, but it is instead split up while the latter has a negligible tuning range, because the peaks of both vanadates are at 1064 nm. Binary oxides are simpler to grow but the alloys must be single phase. As a counter example, alloying Y₂O₃ and Al₂O₃ leads to a variety of different phases (e.g., YAG) with different crystal structures, refractive indices, and emission spectra for each phase.

The ability to continuously tune the composition and properties of the α -(Al_{1-x}Ga_x)₂O₃ during MBE growth without phase changes makes this material well suited

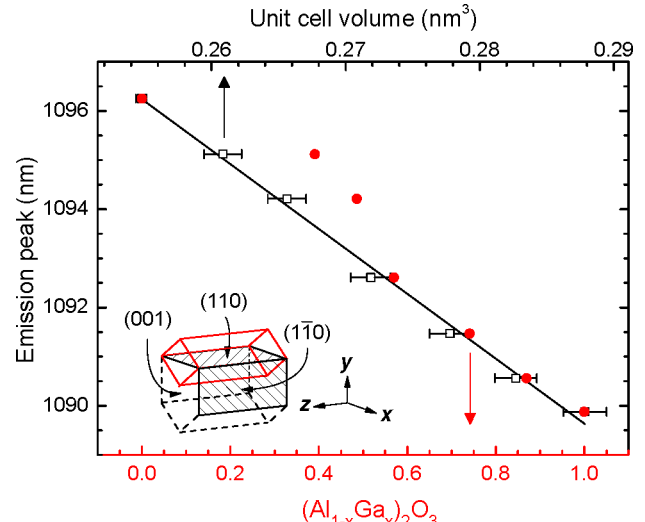


Fig. 4. (Color online) Effect of composition and unit cell volume of Nd-doped α -(Al_{1-x}Ga_x)₂O₃ films on emission peak wavelength. Inset, the hexagonal crystal structure of corundum (unit cell in red) showing the orientations of the x , z (in-plane), and y (out-of-plane) directions with respect to the crystal unit cell.

for making graded-index layers. A waveguide laser using a symmetrically graded core layer with Nd:α-Ga₂O₃ at the center and Nd:α-Al₂O₃ at the edges would have a 1090–1096 nm broad gain profile useful for a tunable laser. Grading the core–cladding interface on either side of the high-index Nd:α-Ga₂O₃ core would be useful for minimizing the scattering losses due to interfacial roughness. We expect a significant improvement over the typical losses of 1 dB/cm observed from other growth methods [1].

In conclusion, we have grown single-crystal films of Nd:α-(Al_{1-x}Ga_x)₂O₃ in the corundum phase by MBE. These alloys are potentially useful as the active waveguiding layer in a planar waveguide laser structure grown on sapphire substrates. The wavelength of the dominant emission peak in the alloy can be adjusted from 1090 to 1096 nm by changing the Ga/Al ratio.

References

1. J. Mackenzie, IEEE J. Sel. Top. Quantum Electron. **13**, 626 (2007).
2. M. Pollnau and Y. E. Romanyuk, C. R. Physique **8**, 123 (2007).
3. R. Kumaran, S. E. Webster, S. Penson, W. Li, T. Tiedje, P. Wei, and F. Schietekatte, Opt. Lett. **34**, 3358 (2009).
4. R. Kumaran, S. Webster, S. Penson, W. Li, and T. Tiedje, J. Cryst. Growth **311**, 2191 (2009).
5. M. Marezio and J. P. Remeika, J. Chem. Phys. **46**, 1862 (1967).
6. R. Moncorgé, in *Spectroscopic Properties of Rare Earths in Optical Materials* (Springer, 2005), pp. 320–378.
7. X. Tang, Z. Ding, and Z. Zhang, in *Proceedings of the 2005 International Conference on Luminescence and Optical Spectroscopy of Condensed Matter* (2007), pp. 66–69.
8. B. M. Walsh, N. P. Barnes, R. L. Hutcheson, R. W. Equall, and B. D. Bartolo, J. Opt. Soc. Am. B **15**, 2794 (1998).
9. Y. Yu, J. Wang, H. Zhang, H. Yu, Z. Wang, M. Jiang, H. Xia, and R. I. Boughton, J. Opt. Soc. Am. B **25**, 995 (2008).